

ments, lanthanum and lutetium. This result for R_{sd} is in contrast to the shielding effect for the $4f$ ground state ($R_{4f} \sim +0.2$) which was previously obtained in Ref. 2, and which is also in agreement with the experimental determinations⁴ for the $4f$ electrons.

Finally, the results for Li $2p$ and $3p$, and for Be $2p$ indicate a small shielding effect ($R \sim 0.1$), and place an upper limit on the correction factors $c = 1/(1-R)$ to be applied to the values of Q derived from the hyperfine structure of these states.

ACKNOWLEDGMENTS

I wish to thank Dr. R. F. Peierls for programming the inward integration of Eq. (5) and the double integral of Eq. (25) for the CDC-6600 computer. Without these programs, the present calculations for Be and Cu would not have been possible in the limited time available. I am also indebted to Dr. H. Bucka, Dr. A. Lurio, Dr. S. Marcus, and Dr. R. Novick for helpful discussions, and to Dr. H. Hühnermann for correspondence.

Optical Emission Produced by Proton and Hydrogen-Atom Impact on Nitrogen*

DUANE A. DAHLBERG,† D. KENT ANDERSON, AND IRVING E. DAYTON

Montana State University, Bozeman, Montana

(Received 30 June 1967)

Optical emissions produced in collisions of protons and hydrogen atoms incident on nitrogen molecules were studied in the spectral region from 1200 to 6000 Å. Relative emission cross sections were measured in the energy range from 10 to 130 keV. The prominent features of the nitrogen spectrum below 2000 Å were the Lyman- α line and atomic nitrogen lines. The Lyman-Birge-Hopfield system appeared also, but it was weak. At the longer wavelengths, the N_2^+ first negative and the N_2 second positive systems dominated the spectrum. Relative emission cross sections for the production of the first negative bands in collisions of hydrogen atoms with nitrogen molecules were nearly constant as a function of energy, and at an energy of 40 keV the cross section was one-half as large as the cross section for proton collisions. The cross section for the second positive band due to hydrogen-atom impact was about 3×10^{-18} cm² at 25 keV, whereas for proton impact the cross section was about 2×10^{-19} cm² at its maximum value. The cross sections for the atomic nitrogen lines produced in hydrogen-atom impact were approximately 75% of the cross sections for the same lines produced in proton impact. Hydrogen-atom collisions had higher cross sections throughout the energy range for the production of Lyman- α emission.

INTRODUCTION

ONE method for studying collisions between two systems is to measure the photon energy which is emitted in optical transitions resulting from the collision. For particular cases, a measurement of the photon emission provides a direct means of obtaining cross sections for exciting atomic and molecular states. A comparison of these experimentally obtained excitation cross sections with theoretical predictions can assist in understanding collision mechanisms.

Atmospheric research indicates that fast protons are entering the atmosphere and contribute to the production of auroras.¹ Because of the charge-exchange process whereby protons pick up electrons from atmospheric gases, there would also be fast hydrogen atoms present. It is evident from the work of Allison and others² that

the equilibrium fraction of hydrogen atoms produced in charge exchange is significant for projectile energies of a few keV to 100 keV. It is of interest, therefore, to determine the effectiveness of the hydrogen atoms in exciting the atmospheric gases and also their contribution to the auroras. The knowledge of hydrogen-atom excitation cross sections is also important in studying the history of a proton entering the atmosphere.

For these reasons optical emissions produced in collisions of protons and hydrogen atoms with nitrogen molecules have been studied. Spectral scans of the light emitted in the collisions of protons with nitrogen gas in the spectral region from 1200 to 6000 Å indicated which transitions of the molecules, of the atoms and ions originating from molecular dissociation, and of the incident particle produced sufficient light intensities for emission cross-section measurements. The results of the scans led to relative emission cross-section measurements for the production of the N_2^+ first negative band system ($B^2\Sigma_u^+ - X^2\Sigma_g^+$), the N_2 second positive band system ($C^3\Pi_u - B^3\Pi_g$), atomic and ionic nitrogen lines, and the Lyman α line. The emission cross sections

* Supported in part by the National Aeronautics and Space Administration under the Sustaining University Program, Grant No. NsG-430.

† National Science Foundation Science Faculty Fellow on leave from Concordia College, Moorhead, Minnesota.

¹ A. B. Meinel, *Astrophys. J.* **113**, 50 (1951).

² S. K. Allison, *Rev. Mod. Phys.* **30**, 1137 (1958).

for these molecular vibrational bands and atomic lines were measured as a function of projectile energy from 10 to 130 keV. Both protons and hydrogen atoms were used as the incident particles.

Optical emissions produced by protons incident on nitrogen have been studied in the visible and near uv spectral region by a number of researchers.³⁻⁶ Some emission cross-section measurements for Lyman- α radiation produced in proton collisions with nitrogen molecules have also been reported.^{7,8} The new results presented in this paper are the emission cross sections for hydrogen atoms incident on nitrogen molecules and the emission studies and cross-section measurements in the vacuum uv spectral region from 1200 to 3000 Å.

APPARATUS

The proton beam from a Cockcroft-Walton accelerator equipped with an rf ion source was focused and mass analyzed. As shown in Fig. 1, the resulting beam passed through a set of collimating apertures in the charge-exchange cell, then into a differentially pumped region, and finally into the excitation chamber. The protons were collected in a Faraday cage at the end of the excitation chamber. If a hydrogen-atom beam was desired, a molecular gas was admitted to the charge-exchange cell. In passing through the charge-exchange cell the initial proton beam became a mixture of hydrogen atoms and protons. The protons were electrostatically deflected from the beam in the differentially pumped region, and the metastable hydrogen atoms were quenched by the deflection field, which left only the ground-state hydrogen atoms to enter the excitation chamber. The hydrogen-atom beam current was measured by secondary-emission techniques. The light which was emitted in the collisions between the incident particle beam and the target gas was chopped mechanically and spectrally analyzed with a monochromator. A photomultiplier and a phase-sensitive detection system were used to measure the light intensity. The MKS Baratron pressure meter was used as the standard pressure measuring device for the majority of the measurements.

Two different monochromators and two different photon detectors were used for analyzing and measuring the intensity of the optical emissions. In the visible and near-uv spectral region, a Bausch and Lomb $\frac{1}{4}$ -m grating monochromator was used in conjunction with an

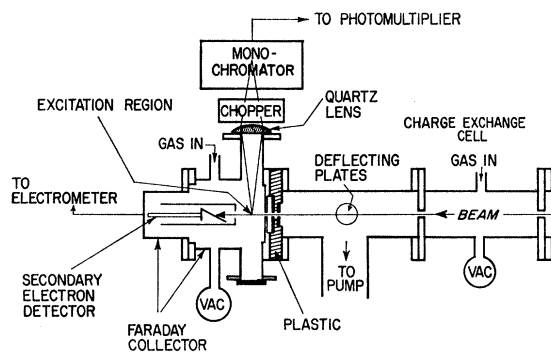


FIG. 1. A view of the section of the apparatus which has direct significance to the experiment.

EMI 9558 QB photomultiplier. The light was focused on the slits of the monochromator with a quartz lens mounted on the excitation chamber. The monochromator was orientated so that the entrance slit was perpendicular to the direction of the proton beam. In the vacuum uv spectral region a McPherson 0.3-m vacuum monochromator with Czerny-Turner optics was used in conjunction with either a Bendix magnetic electron multiplier or the EMI photomultiplier. The electron multiplier was useful below 1250 Å where the photon efficiency of the metal cathode was sufficiently large. Above 1250 Å the photomultiplier with a thin film of sodium salicylate served as the photon detector. Because of the three reflecting surfaces of the McPherson monochromator, the spectral region below 1150 Å could not be studied. The vacuum monochromator was attached directly to the excitation chamber so that the slits of the monochromator could be placed as close as possible to the incident particle beam in order to gain maximum light intensities. The excitation chamber used in the vacuum uv work is shown in Fig. 2. The chamber was constructed so that a window could be used to isolate the chamber from the monochromator.

The width of the entrance slit of the monochromator was always adjusted to be the same as the width of the exit slit. The slit widths were set so that the emissions from transitions near the one being studied could be considered negligible. The actual slit widths used in the experimental work varied with the monochromator used and the transition that was studied.

A beam detector capable of measuring both the proton current and the hydrogen-atom current was

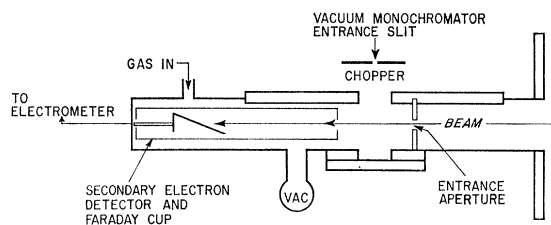


FIG. 2. A schematic of the excitation chamber used in the vacuum uv spectral work.

³ N. P. Carleton and T. R. Lawrence, *Phys. Rev.* **109**, 1159 (1958).

⁴ W. F. Sheridan, O. Oldenberg, and N. P. Carleton, in *Proceedings of the Second International Conference on the Physics of Electronic and Atomic Collisions*, University of Colorado, 1961 (W. A. Benjamin, Inc., New York, 1961), p. 159.

⁵ J. L. Philpot and R. H. Hughes, *Phys. Rev.* **133**, A107 (1964).

⁶ M. Dufay *et al.*, *Compt. Rend.* **261**, 1935 (1965).

⁷ G. H. Dunn, R. Geballe, and D. Pretzer, *Phys. Rev.* **128**, 2200 (1962).

⁸ J. S. Murray, S. J. Young, and J. R. Sheridan, *Phys. Rev. Letters* **16**, 440 (1966).

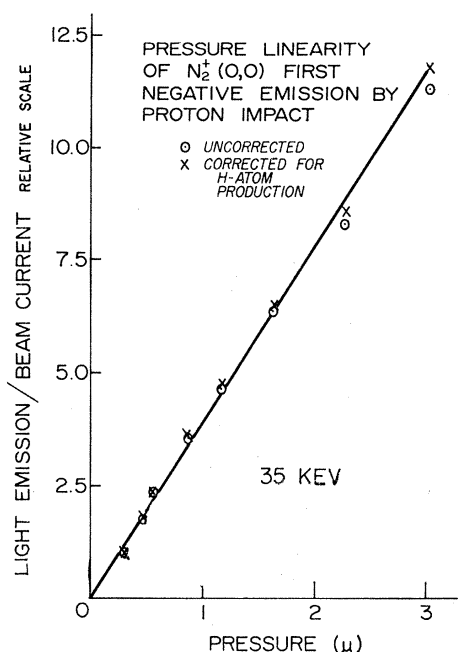


FIG. 3. Light intensity/incident proton as a function of pressure for the production of the (0,0) band of the N_2^+ first negative system.

necessary in this work. This detector consisted of a cylindrical tube with a $\frac{1}{4}$ -in. entrance aperture which enclosed a molybdenum target called the emitter. When measuring proton current, the emitter and enclosure were electrically connected and the detector acted as a Faraday cage. The Faraday cage was effectively a deep, small-diameter cup which essentially trapped the secondary electrons produced in the collision of the protons with the cage. When a negative potential of from 45–90 V was applied to the target and the cylindrical enclosure grounded, the system was a secondary-emission detector. The fact that the molybdenum target made a small angle with the direction of the beam decreased the probability of the secondary electrons being scattered through the entrance aperture of the detector.

In order to calibrate the detector for measuring i' the hydrogen-atom current, the number of electrons emitted per proton colliding with the target N was required as a function of proton energy. To obtain N , the detector was first used as a Faraday cage to measure the current i due to protons entering the collector. Second, the detector was used to measure the secondary electron current i_s emitted from the target under proton bombardment. Finally, N is given by the ratio i_s/i . Stier, Barnett, and Evans⁹ have measured the ratio of N'/N as a function of incident particle energy where N' is the number of electrons emitted per hydrogen atom colliding with the target. From these ratios and mea-

sured values of N, N' could, therefore, be calculated as a function of energy. The hydrogen-atom current was obtained by measuring i_s' for the hydrogen-atom beam and using the calculated values of N' ; then $i' = i_s'/N'$.

The excitation chamber used in the visible spectral region was electrically isolated from the other sections of the system. The entire chamber, therefore, served as a Faraday cage and was used to measure the proton current. The proton currents ranged from 1 μA at 15 keV to 12 μA at 100 keV.

PROCEDURE

Before the cross-section measurements were begun, the spectrum was scanned to observe which transitions produce sufficient emission to permit a detailed study. The scans also assisted in measuring the approximate ratios of intensities of the transitions. Scans were made of the emission produced from protons incident on nitrogen gas in the spectral range from 1200 to 6000 Å. Since higher pressures were required for this work there was some electron and hydrogen-atom excitation present. For example, in the spectral scans of the N_2^+ first negative system and the N_2 second positive system, the major contributions to the second positive bands were from hydrogen atoms produced by electron capture in the target gas and from secondary electrons produced in the collision of the beam with the target molecules.

In the process of taking data, both current and pressure linearity were checked. The linearity of the emitted light intensity per incident particle I/i as a function of the target gas pressure p is important since it is used

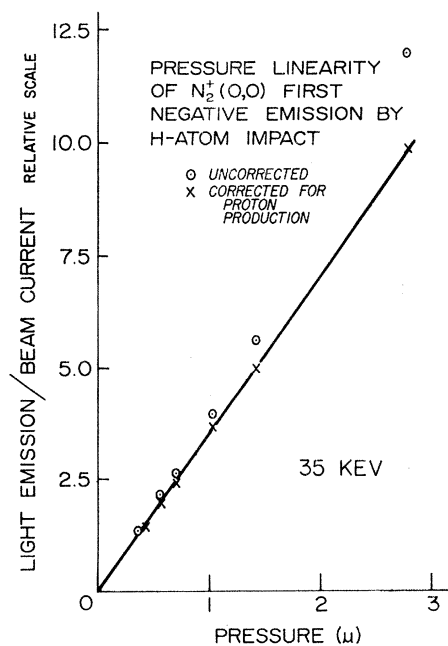


FIG. 4. Light intensity/incident hydrogen atom as a function of pressure for the production of the (0,0) band of the N_2^+ first negative system.

⁹ P. M. Stier, C. F. Barnett, and G. E. Evans, Phys. Rev. 96, 973 (1954).

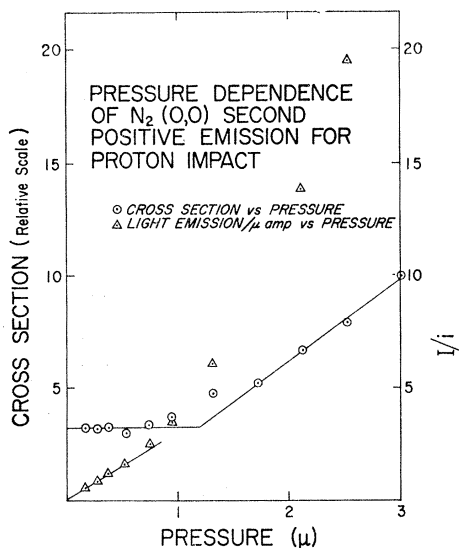


FIG. 5. Light intensity/incident proton and relative cross section as a function of pressure for the production of the (0,0) band of the N_2 second positive system.

as the criterion for determining the source of optical emissions. If the emitted light results from collisions between the primary incident particles and the target gas, the emission cross section Q will be proportional to $I/i\bar{p}$, and I/i will be a linear function of pressure. If the emitted light results from collisions between secondary particles and the target gas, Q will be proportional to $I/i\bar{p}^2$ and there will be a quadratic dependence of I/i on pressure.

For the emissions from the N_2^+ first negative vibrational transitions, measurements of I/i as a function of \bar{p} from about 0.3 to 5 μ were made at a number of different energies and they all revealed a linear relationship, indicating that the emissions were produced by the primary particles. The two sets of data for the (0,0) vibrational transitions taken at 35 keV are shown in Figs. 3 and 4. In the proton-impact work a correction was required for hydrogen-atom production. A correction was also required for the proton production in the hydrogen-atom data. These corrections are shown in Figs. 3 and 4.

For the $N_2(0,0)$ second positive vibrational band, measurements of I/i as a function of pressure were made at a number of different incident-particle energies. For hydrogen-atom impact a linear relationship of I/i as a function of pressure existed, but only for pressures under 5 μ . The authors attributed the nonlinear relationship to the emission caused by secondary electrons produced in the collisions of the incident particles with the target gas. In the case of proton excitation, however, the relationship between I/i and pressure is more complex. Both secondary electrons and also hydrogen atoms in the beam produced by electron capture contribute to the emission. Figure 5 presents a graph of both relative cross section as a function of pressure and

I/i as a function of pressure at a proton energy of 43 keV. From these data, the authors concluded that the emission due to the primary particles was masked by emissions due to secondary particles at pressures above 2 μ . To obtain data for the excitation of the $N_2(0,0)$ band by fast protons, it was, therefore, necessary to work at pressures around 1 μ .

I/i as a function of the target gas pressure from about 0.5 to 10 μ was measured for each of the other transitions studied. Each of these revealed a linear relationship between I/i and \bar{p} , indicating the experimental conditions were such that the observed emissions were due to the primary particles.

The mass-analyzed projectile beam entering the excitation chamber was always a mixture of a hydrogen-atom current i' and a proton current i . The ratio of i'/i was a function of both the gas pressure in the exchange cell \bar{p}' and the energy E of the initial proton beam. As \bar{p}' was increased the ratio of i'/i also increased. According to the charge-exchange cross sections, as E was increased the ratio of i'/i decreased rapidly.²

The experimental problem was to distinguish the emission produced in the collision of the hydrogen atom with the target gas from the emission produced in the collision of the proton with the target gas. In order to separate these emissions ($I+I'$), ($i+i'$), and i were measured for \bar{p}' at background pressure and at a selected value of E , where I and I' were, respectively, the measured light intensity due to the collision of the protons with the target gas and measured light intensity due to the collision of the hydrogen atoms with the target gas. The protons were then deflected out of the beam leaving only the hydrogen atoms to produce emission. At this point I' and i' were measured. The preceding procedure was repeated for the same value of E and for one or more values of \bar{p}' . For each of the measurements, the target-gas pressure was recorded also. Since I and I' were related to the total emission produced in proton and hydrogen-atom collisions, respectively, and \bar{p} was proportional to the target-gas density, the quantity $I'/i'\bar{p}$ is the relative emission cross section for the hydrogen-atom collisions, and $I/i\bar{p}$ is the relative emission cross section for the proton collisions. Repeating the measurements and calculations for a number of values of E between 10 and 130 keV gave relative emission cross sections as a function of energy.

Values of \bar{p} from 0.5 to 3.0 μ were used in these emission cross-section measurements. In measuring the relative cross sections for a single line or band, \bar{p} was held to changes of less than 10% for all values of E .

The emitted light intensity was not absolutely calibrated by the authors. Absolute values for the cross sections were obtained by normalizing some of these measured relative cross sections to absolute measurements made by other researchers. These normalization procedures will be discussed with the results.

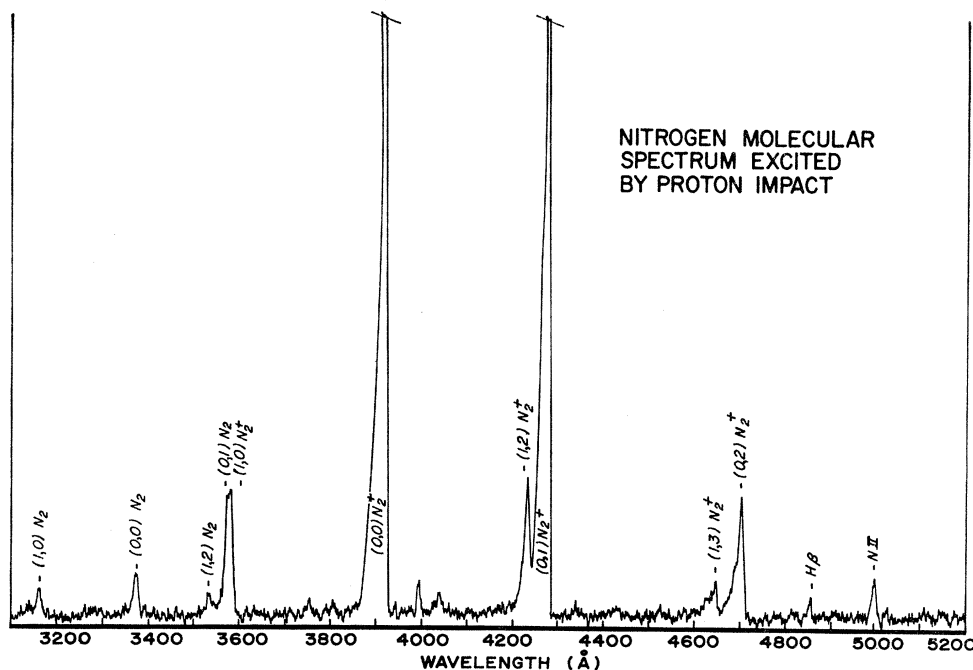


FIG. 6. Spectrum produced by a 7- μ A beam of 55-keV protons incident upon nitrogen gas at a pressure of 5.7 μ . Monochromator slits equivalent to 7 \AA .

RESULTS

From the spectral scans for protons incident on nitrogen molecules (see Fig. 6), one observes that above 2000 \AA the vibrational bands of the N_2^+ first negative system ($B^2\Sigma_u^+ - X^2\Sigma_g^+$) are dominant. Some of the bands of the N_2 second positive system ($C^3\Pi_u - B^3\Pi_g$) and two ionic nitrogen lines appeared also. In addition, the Balmer lines of hydrogen produced in the electron capture process were present. In the spectral region below 2000 \AA (see Fig. 7), atomic nitrogen lines and Lyman- α were the most prominent emissions of the spectrum. The forbidden bands of the Lyman-Birge-Hopfield system ($a^1\Pi_g - X^1\Sigma_g^+$) appeared, but their intensity was significantly weaker than the intensity of the atomic lines. Of interest, also, was the appearance of the unidentified band at 1589 \AA reported by Carroll.¹⁰

N_2^+ First Negative System

The (0,0), (0,1), (0,2), (1,3) bands at 3914, 4278, 4709, 4652 \AA , respectively, of the N_2^+ first negative system were selected for cross-section measurements. Measurements were made for both proton and hydrogen-atom impact. The emission due to the (1,0) band could not be measured for hydrogen-atom impact because of the nearness of the (0,1) band of the second positive system.

After all corrections were made, the (0,0) emission cross sections due to proton impact were normalized to the absolute measurements of Philpot and Hughes.⁵ Since the relative measurements of this work had the same energy dependence over the energy interval of

40 to 70 keV as Philpot and Hughes's measurements, the normalization was made in this energy region. The hydrogen-atom data were then normalized to the proton work of this paper. Emission cross sections for the other bands were also normalized to the (0,0) proton-impact cross sections. Corrections were made only for the variation in the spectral response of the monochromator. The final results are presented in Fig. 8.

From these curves of cross section as a function of energy, it is observed that the curves for transitions originating from the $v'=0$ level have the same shape. This characteristic holds for both the proton-impact data and the hydrogen-atom-impact data. Since these transitions all originate from the same upper state, and the transition probabilities are independent of the means of exciting the particular level, the shapes are in fact expected to be the same.

The (1,3) band is the only one which originates from a level different from the $v'=0$ for which emission cross sections by hydrogen-atom impact could be measured. These data reveal that the ratio of Q_0/Q_+ appears to be somewhat greater for exciting the $v'=1$ level than for exciting the $v'=0$ level, where Q_0 and Q_+ are, respectively, the emission cross sections for hydrogen impact and for proton impact.

The effectiveness of the hydrogen atom in exciting transitions in the first negative system reveals little energy dependence over the energy region of these measurements. It does reveal, however, that the hydrogen-atom excitation of the $v'=0$ level is a significant fraction of the proton excitation, especially at the higher energies. The ratio of Q_0/Q_+ is $\frac{1}{2}$ at 40 keV and $\frac{2}{3}$ at 90 keV.

¹⁰ P. K. Carroll, Can. J. Phys. **36**, 1585 (1958).

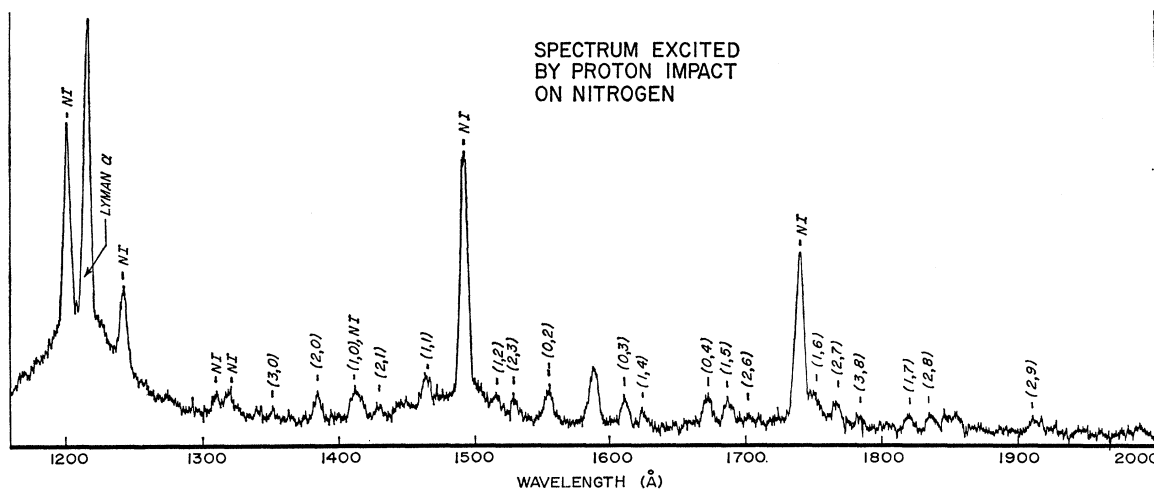


FIG. 7. Spectrum produced by a $10\text{-}\mu\text{A}$ beam of 55-keV protons incident on nitrogen gas at a pressure of 25μ . Monochromator slits equivalent to 4 \AA .

The relationship of emission to excitation for the first negative system is easily obtained since the upper state is populated only by direct excitation and not by cascading. The $C^2\Sigma_u^+$ state which lies above the B state of N_2^+ would not be expected to populate the B state for two reasons. First, the transition between the two states is forbidden. Second, the Franck-Condon principle predicts that the levels of the C state that are most likely to be excited, predissociate.¹¹

The cross sections for the excitation of the $v'=0$ level can then be obtained by measuring the emission cross sections for each of the bands originating from the $v'=0$ level and summing the results. In this case, a fair approximation is the sum of emission cross sections for the (0,0), (0,1), and (0,2) transitions, since the relative intensities of transitions to states with $v'' > 2$ are small.

N₂ Second Positive System

Emission cross sections were measured for the (0,0) transition of the second positive system at 3371 \AA . These curves are displayed in Fig. 9. The low light intensities and the stringent pressure requirements prevented measurements of other bands in this system.

As in the case of the first negative system, these data were normalized to the (0,0) band of the first negative system correcting only for the change in spectral efficiency of the monochromator.

The data reveal an emission cross section due to hydrogen-atom impact that decreases rapidly with increasing energy, showing no sign of a peak even for the lowest energy at which measurements were made. The emission cross section for proton impact reveals a very small probability of excitation of the upper state of this system. The statistics were quite poor at low energies, which left considerable uncertainty in the

shape of the cross-section curve for proton impact at these energies. There does, however, appear to be a maximum in the curve at about 35 keV.

No known states exist above the $C^3\Pi_u$ state which would be expected to populate this state by cascading. The emission resulting from the C state was considered to be entirely due to the direct excitation of this state. The emission from the (0,0) band is, therefore, directly proportional to the probability of excitation of the $v'=0$ level of the C state.

Atomic and Ionic Nitrogen Lines

Proton- and hydrogen-atom-impact data for the N I lines produced by the $3s^2P-2p^2P^0$ and the $3s^2P-2p^2D^0$

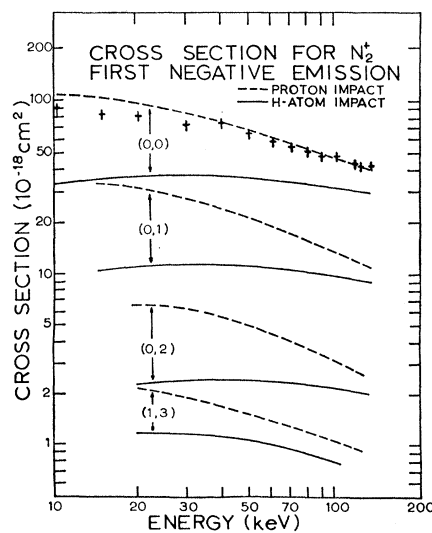


FIG. 8. Cross section for the production of the N_2^+ first negative emission system by proton and hydrogen-atom impact. Normalization was made to the absolute cross sections for proton impact measured by Philpot and Hughes (see Ref. 5).

¹¹ P. K. Carroll, Can. J. Phys. **37**, 880 (1959).

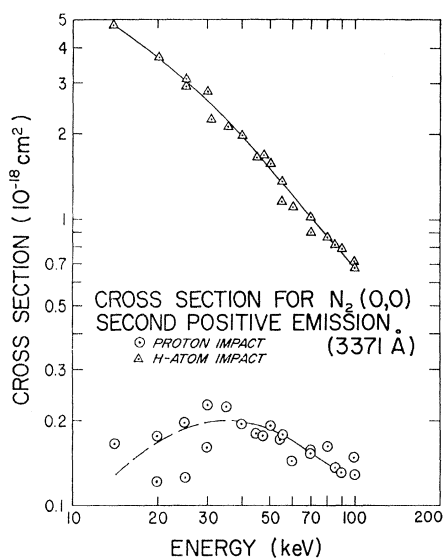


Fig. 9. Cross section for the production of the (0,0) band of the N_2 second positive system by proton and hydrogen-atom impact.

transitions at 1743 and 1493 Å, respectively, and the $N II$ line produced by the $3d^3F^0-3p^3D$ transition at 5005 Å are shown in Figs. 10 and 11. The cross-section data for the $3s^4P-2p^4S^0$ transition at 1200 Å are not shown because the closeness and the Doppler broadening of the Lyman- α line did not permit meaningful measurements of this line. The emission by proton impact from the $N II$ transition has been measured and reported.^{5,6}

An absolute determination of the emission cross section for the $N II$ line was accomplished by normalizing these data to the proton cross-section data for the $N_2^+(0,0)$ first negative emission, correcting only for the spectral response of the monochromator.

Absolute values for emission cross sections of the atomic lines were more difficult to obtain because of the wavelength region in which these lines are located. As will be discussed later, the Lyman- α data were normalized to the measurements of Van Zyl.⁸ The cross-section measurements for the $N I$ line could, therefore, be normalized to these Lyman- α data. To obtain absolute values for the two lines, the assumption was made that the spectral efficiency of the monochromator was essentially the same for Lyman- α at 1216 Å as for the $2P-2P^0$ transition at 1743 Å, since the grating was blazed for 1500 Å. This assumption introduces an additional uncertainty of possibly 50%. Then, the absolute determination for the $2P-2D^0$ line was accomplished from the knowledge of the transition probabilities for the $2P-2P^0$ and $2P-2D^0$ transitions.¹² It is assumed that the transition probabilities for transitions from the same upper state are independent of the method of excitation.

¹² P. S. Kelly, *Astrophys. J.* **140**, 1247 (1964).

These data reveal that the atomic-nitrogen emission curves produced by proton impact have maxima somewhere around 25 keV. For hydrogen-atom impact the peaks are not clearly defined because of the statistics. There is, however, very little difference in the magnitudes of excitation by proton impact and hydrogen-atom impact. At the lower energies, Q_0/Q_+ is about $\frac{3}{4}$ and increases with increasing energy.

No corrections were made for the populating of the upper states by cascading from higher levels in any of the cross-section measurements for the atomic and ionic emissions. Without cross-section measurements

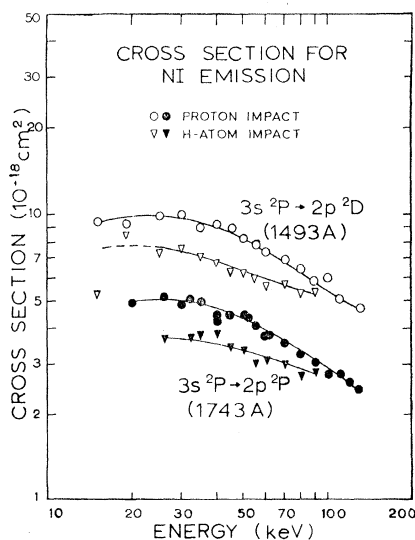


Fig. 10. Cross section for the emission of $N I$ multiplets from the $3s^2P$ state.

for lines in the longer-wavelength spectral region, it is impossible accurately to account for the cascading effect.

Lyman- α Line

There are two basic problems associated with measuring the excitation of the fast particle. One is to account for the populating of states by cascading from higher levels. The second is to account for the change in emission as a function of path length due to the finite lifetimes of the excited states.

The ideal conditions are an equilibrium between excitation and emission, and a knowledge of the emission cross sections of all the states. The equilibrium condition, however, requires path lengths on the order of meters. If the beam traveled distances of meters in the target gas, the composition of the beam would no longer be known unless very low pressures were used. The light intensities at such pressures would be too weak for measurements by the techniques used for this work. An important factor in the Lyman- α measurements is the presence of atomic nitrogen lines nearby.

Since there is a strong N I line at 1200 Å and a weaker line at 1243 Å, monochromator slits equivalent to 8 Å were necessary for the Lyman-α measurements.

For these reasons some sort of compromise was required. The experimental conditions of this work provided what appeared to be the best compromise. The technique was to observe the optical emission very soon after the beam entered the excitation chamber. If the lifetimes of the states capable of populating the 2p state by cascading were sufficiently long, the hydrogen atoms in these states would have passed the region of observation before emitting their radiation. If the lifetime of the 2p state were sufficiently short, an equilibrium between the direct excitation to, and the emission from, the 2p state could then be established. Since a range of particle velocities was used in this work, the optimum condition was not possible for the entire energy range. The error was estimated to be less than 20%. Further experimental work and refinement of the apparatus is necessary in order to determine the error exactly.

The relative cross sections for the production of Lyman-α as a function of incident particle energy were

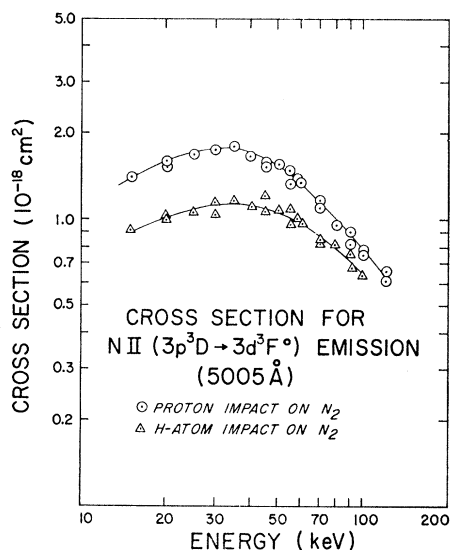


FIG. 11. Cross section for the production of the $3d^3F^0-3p^3D$ N II line by proton and hydrogen-atom impact. The order of the states is reversed in the figure.

measured in the energy range from 20 to 130 keV. These results, which were normalized to the proton impact data of Van Zyl⁸ at 20 keV, are shown in Fig. 12. No correction was made for the possible systematic errors which were discussed previously. The proton-impact curves show a very rapid decrease in the production of Lyman-α as the energy of the proton is increased. The production of Lyman-α by hydrogen-atom impact has a higher cross section over the entire energy range than the cross section for proton impact. One different feature in the hydrogen-atom cross-section curve as compared

TABLE I. Some of the processes resulting from collisions of protons and hydrogen atoms with nitrogen molecules.

Number	Process	Energy defect
1	$H^+ + N_2 - H^0 + N_2^+$	1.9 (eV)
2	$-H^0 + N_2^{*+}$	4.9
3	$-H^+ + N_2^+ + e$	15.5
4	$-H^+ + N_2^{*+} + e$	18.5
5	$H^0 + N_2 - H^0 + N_2^+ + e$	15.5
6	$-H^0 + N_2^{*+} + e$	18.5
7	$-H^+ + N_2^+ + 2e$	29.1
8	$-H^+ + N_2^{*+} + 2e$	32.1
9	$-H^- + N_2^{*+}$	17.7
10	$H^+ + N_2 - H^+ + N_2^*$	11.0
11	$H^0 + N_2 - H^0 + N_2^*$	11.0
12	$H^0 + N_2 - H^+ + N_2^* + e$	24.6
13	$H^0 + N_2 - H^0 + N_2^*$	10.2
14	$H^0 + N_2 - H^0 + N_2^+ + e$	25.7
15	$H^+ + N_2 - H^0 + N_2^+$	12.1
16	$H^0 + N_2 - H^0 + N_2^*$	21.2

with the proton cross-section curve is the apparent abrupt change in the slope occurring at about 45 keV.

DISCUSSION

The processes and the energy defects are presented in Table I as a guide for determining the possible excitation mechanisms.

N₂⁺ First Negative System

Since the excitation produced in conjunction with the charge-exchange process requires less energy than the other processes, the authors expect process 2 to contribute significantly to the excitation in proton impact. If the energy dependence of process 2 is the

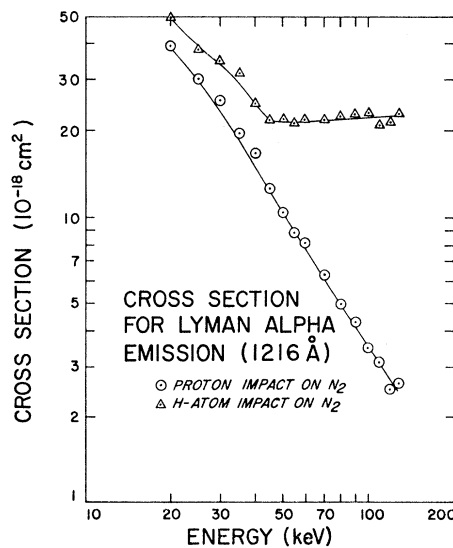


FIG. 12. Cross section for the production of the Lyman-α line by protons and hydrogen atoms incident on nitrogen.

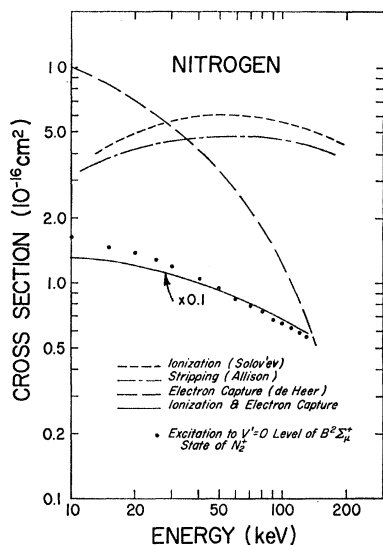


FIG. 13. Cross sections for the ionization of N_2 by proton impact [E. S. Solov'ev, R. N. Il'in, V. A. Oparin, and N. V. Fedorenko, Zh. Eksperim. i Teor. Fiz. 42, 659 (1962) [English transl.: Soviet Phys.-JETP 15, 459 (1962)]], for electron capture of protons incident on N_2 [F. J. DeHeer, J. Schutzen, and H. Maustafa, Physica 32, 1766 (1966)], and for the stripping of hydrogen atoms incident on N_2 (see Ref. 2). Cross sections also for the sum of ionization and electron capture compared with the excitation of the $v'=0$ level of the $B^2\Sigma_g^+$ state of N_2^+ produced by protons incident on N_2 .

same as the energy dependence of process 1, process 2 cannot, however, explain the observed energy dependence of the first negative system. As is shown in Fig. 13, the charge-exchange cross section decreases much more rapidly than the emission measurements of this work. If one adds the ionization cross section to the charge-exchange cross section, the result is a curve which has about the same shape as the cross-section curve for the

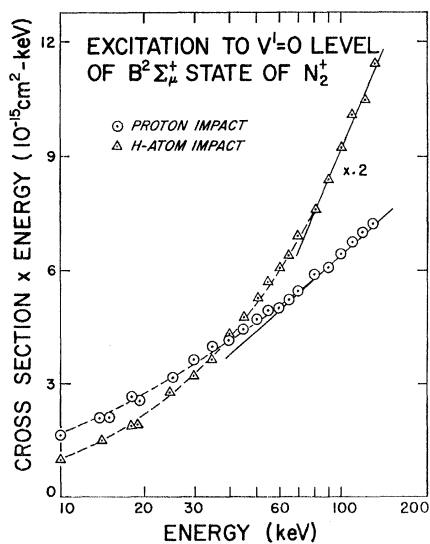


FIG. 14. Cross section for the excitation of the $v'=0$ level of the N_2^+ first negative system by proton and hydrogen-atom impact plotted in terms of QE as a function of $\ln E$.

excitation of the $v'=0$ level of the B state. This comparison is also shown in Fig. 13. Now, if the energy dependence of the sum of processes 1 and 3 has the same energy dependence as the sum of the processes 2 and 4, there is justification for believing that both processes 2 and 4 contribute to the observed emission.

The curve of the sum of processes 1 and 3 is approximately a measure of the total cross section for the production of N_2^+ . The experimental curve is a measure of the cross section for the excitation of the $v'=0$ level of the B state of N_2^+ . The ratio of these curves would, therefore, approximately represent the fraction of the molecular ions excited to the $v'=0$ level to the total number of molecular ions formed. This fraction is on the order of 0.1.

With reference to the processes listed, the simple ionization and excitation of N_2 requires the least amount of energy for exciting the B state in hydrogen-atom im-

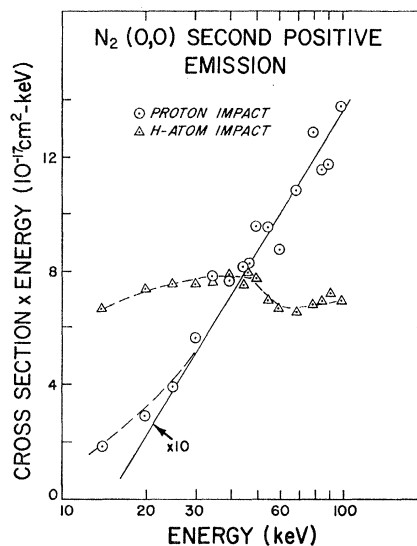


FIG. 15. Cross section for the production of the (0,0) band of the N_2 second positive system by proton and hydrogen-atom impact plotted in terms of QE as a function of $\ln E$.

pact. If the collision were more violent, the hydrogen atom could also be excited or ionized leading to process 8. This process, however, requires approximately twice the energy of process 6. Since the cross section for electron capture by the hydrogen atom is small, process 9 is not expected to contribute significantly at these energies.

At high energies, the energy dependence of the cross section can be predicted by the Bethe-Born approximation for some processes. The cross section is expected to have an $(1/E)\ln E$ dependence for electric dipole transitions and an $1/E$ dependence for an electric quadrupole transition, where E is the incident-particle energy. By plotting QE as a function of $\ln E$, the functional form of the energy dependence can most easily be exhibited. The graph of QE as a function of $\ln E$

for proton impact (see Fig. 14), indicates an apparent $(1/E) \ln E$ dependence of Q at the higher energies. For hydrogen-atom impact also a linear region is apparently being approached at the higher energies.

N₂ Second Positive System

For hydrogen-atom impact, process 11 would appear the more likely because of the smaller amount of energy required. This direct-excitation process, however, would not be expected to excite a triplet state from a singlet ground state unless electron exchange were involved. If the hydrogen atom is stripped of its electron in the interaction, process 12 would result. Even though this process requires an additional energy of 13.6 eV it represents a possible mechanism. In Fig. 15 the curve of QE plotted as a function of $\ln E$ does not show the linear behavior indicative of a simple dipole transition at the higher energies. The excitation mechanism, therefore, is more complex, and the structure in the curve complicates the situation even more. Referring to Fig. 9, the rapid decrease of cross section with energy would predict an exchange mechanism.¹³ Hydrogen-atom excitation has not been extensively studied, but in the work of Van Eck *et al.*,¹⁴ their conclusion is that electron exchange accounts for the excitation of the triplet states of helium.

In the case of proton impact, spin-conservation rules do not allow excitation of a pure triplet state.¹⁵ Since excitation of the C state is observed for proton impact, there must be some mechanism permitting the excitation. The curve of QE as a function of $\ln E$ (see Fig. 15), indicates that, in spite of the rather poor statistics, there is the definite $(1/E) \ln E$ dependence predicted for a simple dipole excitation. If spin-orbit coupling were present, the C state could be a mixture of both singlet and triplet terms. This mixing would then allow for some excitation of the C state by proton impact. The process responsible for the observed emission would then be a simple excitation of the nitrogen molecule. In their studies of electron impact on nitrogen, Lassette *et al.*¹⁶ claim that the C state is a linear combination of singlet and triplet terms. The singlet element is considered to be small but present. In the absorption spectrum of nitrogen, Tanaka¹⁷ observed bands having intensities nearly as great as the $L-B-H$ bands which he attributed to $C^3\Pi_u-X^1\Sigma_g^+$ transitions.

Atomic and Ionic Lines

In collisions, there are a number of mechanisms for producing as final products either an excited nitrogen

¹³ *Atomic and Molecular Processes*, edited by D. R. Bates (Academic Press Ltd., London, 1962), Chap. 14.

¹⁴ J. Van Eck, F. J. DeHeer, and J. Kistemaker, *Physica* **30**, 1171 (1964).

¹⁵ E. Wigner, *Nachr. Ges. Wiss. Göttingen. Jahresber. Geschäfts-jahr; Math.-physik Kl., Fachgruppen II*, 375 (1927).

¹⁶ E. N. Lassette, A. Skerbele, and V. D. Meyer, *J. Chem. Phys.* **45**, 3214 (1966).

¹⁷ Y. Tanaka, *J. Opt. Soc. Am.* **45**, 663 (1955).

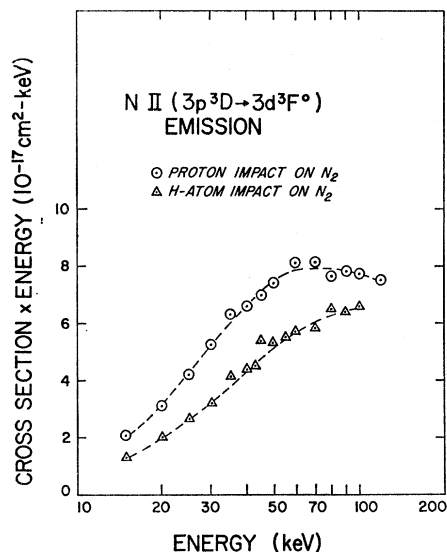


FIG. 16. Cross section for the production of the $3d^3F^0-3p^3D$ N II line by proton and hydrogen-atom impact plotted in terms of QE as a function of $\ln E$. The order of the states is reversed in the figure.

ion or an excited nitrogen atom. Two means of dissociating and exciting the atom to the $3s$ state, or the ion to the $3p$ state will be mentioned. One is to ionize a $\sigma_g 2s$ electron, leaving the molecular ion with about 25 eV of excess energy.¹⁸ The molecular ion could find itself in a dissociative state such that either one or both of the end products was left in highly excited states. The other possibility that will be mentioned involves the interaction of the projectile with more than one electron of the target system. If, for example, two

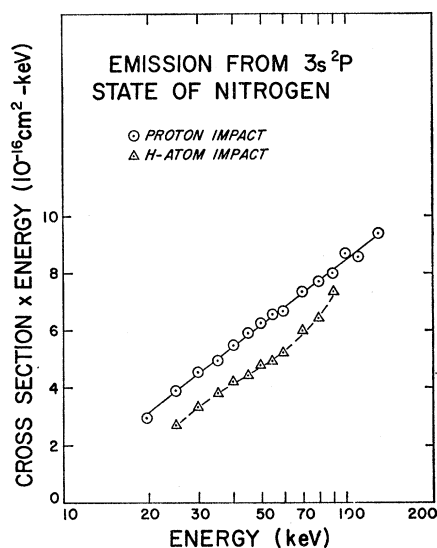


FIG. 17. Total cross sections for emissions from the $3s^2P$ state of nitrogen due to proton and hydrogen-atom impact plotted in terms of QE as a function of $\ln E$.

¹⁸ B. J. Ransil, *Rev. Mod. Phys.* **32**, 239 (1960).

electrons were raised to higher orbitals, and one is ionized by the Auger process, the molecular ion could again be left in a dissociative state capable of producing highly excited products.

As shown in Fig. 16, the graphs of QE as a function of $\ln E$ for the N II emission reveal a rather strange behavior. There appears initially an $(1/E) \ln E$ dependence of the cross section which changes at higher energies to approximately an $1/E$ dependence. Figure 17 displays for both proton and hydrogen-atom impact approximately an $(1/E) \ln E$ dependence for the atomic-nitrogen emission over the entire energy range. This dependence on the energy indicates that the process leading to dissociation of the molecule or molecular ion into excited atoms might be described by the dipole Born approximation.

From the differences in the energy dependences of the N II and the N I emissions, it appears that at high energies the mechanism dominating the production of the N II emission must be different from that of the N I emission.

Further information is possible from the identification of the particular atomic and ionic lines which were present in the spectral scans. Such an identification would indicate the probable states of the dissociation products which produce the observed atomic and ionic emissions. A study of the spectral scans revealed the following transitions:

$3s^4P-2P^4S^0$	1200 Å	N I
$3s^2P-2p^2P^0$	1743	
$3s^2P-2p^2D^0$	1493	
$3s'^2D-2p^2D^0$	1243	
$3s'^2D-2p^2P^0$	1411	
$3d^2P-2p^2P^0$	1319	
$3d^2D-2p^2P^0$	1311	
$3d^3F^0-3p^3D$	5005	N II
$3p^3D-3s^3P^0$	5680.	

The N II line at 5680 Å cannot be seen in Fig. 6, but was observed by the authors in other spectral scans. This line has also been reported by other authors.^{5,6}

It is interesting that the transitions originating from the $3s$ and $3d$ levels of atomic nitrogen are strong, but the transitions originating from the $3p$ and $4p$ levels are not present at all. Three transitions originating from p levels which should appear, but were not observed, are

$3p^2D^0-3s^2P$	4109 Å	N I
$3p^2P^0-3s^2P$	3830	
$4p^2S^0-3s^2P$	4935.	

From these observations it is believed that the dissociation limits of the repulsive states producing the

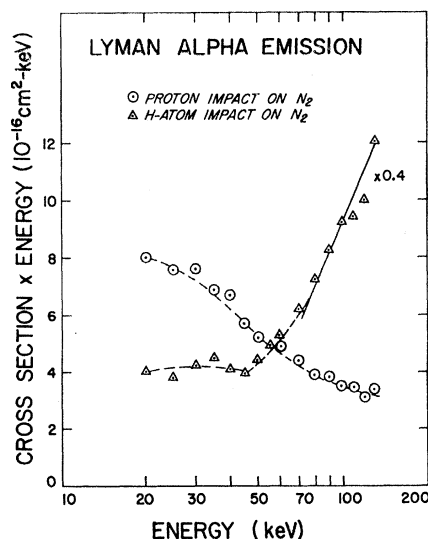


Fig. 18. Cross section for the production of Lyman- α line by proton and hydrogen-atom impact on nitrogen plotted in terms of QE as a function of $\ln E$.

observed emissions are some combinations of $N^+(3d)$, $N^+(3p)$, $N(3s)$, and $N(3d)$.

It is also interesting that emissions from both the $2s^22p^2(^3P)nl$ and the $2s^22p^2(^1D)nl$ families are present in the spectral scans. The ground state of atomic nitrogen is the $4S^0$, indicating that in the lowest energy state the spins of all the $2p$ electrons are parallel. The fact that the two families of excited states are present means that the two $2p$ electrons in the excited atom which results from the dissociation can have their spins either parallel or antiparallel.

In addition to the transitions recorded above, a line has been observed by Dufay *et al.*⁶ at 6482 Å for which cross sections were measured. This line was attributed to atomic nitrogen. There are, however, transitions in both atomic and ionic nitrogen at 6482 Å. In atomic nitrogen the transition is the $4d^4F-3p^4D^0$ and in the ion it is the $3p^1P-3s^1P^0$. From the relative intensities of lines that have been observed here, and from the differences in the energy dependencies of the cross sections for atomic and ionic emissions, there is no definite evidence for the choice of the atomic transition over the ionic transition.

Lyman- α Line

The cross-section curve for Lyman- α emission by proton impact has the same general shape as that of the charge exchange cross-section curve reproduced for reference in Fig. 13. If the errors discussed previously were taken into consideration, the two curves would more nearly have the same shapes. This general relationship between the shapes of the emission curve and the charge-exchange curve is expected since the existence of a hydrogen atom in the beam depends upon the charge-exchange process.

The curve of QE as a function of $\ln E$ (see Fig. 18), is not really applicable to this process since the Born approximation predicts an E^{-6} dependence of cross section for charge exchange. The curve does, however, show that the energy decreases less rapidly than the prediction of the Born approximation. The energy dependence of the cross section is approximately $E^{-1.6}$.

The change in the slope of the curve of cross section as a function of energy, for hydrogen-atom impact (Fig. 12), implies that more than one process contributes to the excitation of the $2p$ state. One possibility is a process A , for which the cross section decreases very rapidly with energy, dominating at the low energies, and a process B for which the cross section is nearly independent of energy, dominating at the high energies.

Experimental data for basic atom-molecule inelastic cross sections are not adequate for making a quantitative analysis of the processes involved in producing Lyman- α emission. On the basis of this work some observations can be made, however. For energies above 45 keV the cross section for Lyman- α emission due to hydrogen-atom impact is almost independent of energy. This behavior is very similar to the stripping cross section in Fig. 13, where the electron is removed from the atom instead of remaining in an excited state. Further, the energy dependence of the cross-section curve plotted in terms of QE as a function of $\ln E$ shown in Fig. 18 seems to be approaching the prediction of the Born approxi-

mation for a simple dipole excitation. Process B could, therefore, be identified with a simple excitation of the hydrogen atom without specifying the final state of the nitrogen molecule. Below 45 keV the rapid decrease of cross section with energy is indicative of an electron-exchange mechanism. Process A , therefore, could be thought of as involving electron exchange.

Comparing the Lyman- α results for hydrogen-atom impact with the emission cross section for the second positive system of N₂ due to hydrogen-atom impact, one notes shapes that are similar for energies less than 45 keV. From Figs. 15 and 18, it is also noted that the breaks in the two hydrogen-atom curves occur at about the same energy. One possible explanation for the break in the cross section for excitation by hydrogen atoms of the N₂ second positive system (Fig. 18) is the conservation of probability. One supposes that this excitation process is coupled via a charge-exchange mechanism to the excitation of Lyman- α in the projectile. At an energy of 45 keV, process B begins to dominate the Lyman- α channel, which in turn affects the N₂ channel. The effect is rather small because of the great number of alternate inelastic channels in the collision.

ACKNOWLEDGMENTS

The authors wish to acknowledge the assistance of A. Romer, E. Teppo, and J. White in taking data.

Theory of Weak Atomic and Molecular Interactions*

J. I. MUSER AND A. T. AMOS†

Belfer Graduate School of Science, Yeshiva University, New York, New York

(Received 5 June 1967)

A new perturbation procedure for calculating interatomic interaction energies in which the wave function is expanded in terms of product functions is presented. The method is used to discuss various difficulties which can arise in such calculations and these are illustrated by considering the problem of the interaction of two hydrogen atoms. It is found that (a) the inclusion of continuum states in the basis set of functions is of vital importance; (b) the inclusion of charge-transfer states or of antisymmetrical product functions in the basis set can lead to ambiguous results; (c) in general, exchange integrals cannot be neglected relative to Coulomb integrals; and (d) only when the basis functions are products of the individual atomic wave functions is it possible to make *a priori* estimates of the magnitudes of the higher-order terms in the perturbation expansion.

I. INTRODUCTION

THE energy of interaction between atoms, molecules, and magnetic ions has long been of interest, since it provides the cohesive energy of rare-gas atomic

and molecular crystals, the spin-dependent energy between sublattices in insulators containing magnetic ions, the mechanism for enhancing forbidden optical transitions, etc. Nevertheless, since the classic paper of Eisenschitz and London,¹ there have been few attempts to treat the problem in a more or less rigorous fashion, most authors having restricted their discussions to the

* Research supported in part by the National Science Foundation.

† Permanent address: Department of Mathematics, University of Nottingham, Nottingham, England.

¹ H. Eisenschitz and F. London, Z. Physik **60**, 491 (1930).